Spectroscopic properties of the 1.4 μm emission of Tm^{3+} ions in TeO_2-WO_3-PbO glasses

R. Balda[1,2*], L. M. Lacha[1], J. Fernández[1,2], M. A. Arriandiaga[3], J. M. Fernández- Navarro[4], and D. Munoz-Martin[4]

[1]*Departamento de Fisica Aplicada I, Escuela Superior de Ingenieros, Alda. Urquijo s/n 48013 Bilbao, Spain*
[2]*Unidad Física de Materiales CSIC-UPV/EHU and Donostia International Physics Center, Apartado 1072, 20080 San Sebastian, Spain*
[3]*Departamento de Fisica Aplicada II, Facultad de Ciencia y Tecnología, Universidad del País Vasco, Apartado 644, Bilbao, Spain*
[4]*Instituto de Optica, Consejo Superior de Investigaciones Científicas, Serrano 121, 28006 Madrid, Spain*
**Corresponding author: wupbacrr@bi.ehu.es*

Abstract: In this work, we report the spectroscopic properties of the infrared $^3H_4 \rightarrow {}^3F_4$ emission of Tm^{3+} ions in two different compositions of glasses based on TeO_2, WO_3, and PbO for three Tm_2O_3 concentrations (0.1, 0.5, and 1 wt%). Judd-Ofelt intensity parameters have been determined and used to calculate the radiative transition probabilities and radiative lifetimes. The infrared emission at around 1490 nm corresponding to the $^3H_4 \rightarrow {}^3F_4$ transition has two noticeable features if compared to fluoride glasses used for S-band amplifiers. On one hand, it is broader by nearly 30 nm, and on the other, the stimulated emission cross section is twice the value for fluoride glasses. Both the relative intensity ratio of the 1490 nm emission to 1820 nm and the measured lifetime of the $^3H_4$ level decrease as concentration increases, due to the existence of energy transfer via cross-relaxation among Tm^{3+} ions. The analysis of the decays from the $^3H_4$ level with increasing concentration indicates the presence of a dipole-dipole quenching process assisted by energy migration.

OCIS codes: (140.3380) Laser Materials; (160.5690) Rare earth doped materials; (300.6280) Spectroscopy, fluorescence and luminescence

References and links

1. J. Y. Allain, M. Monerie, and H. Poignant, "Tunable cw lasing around 0.82, 1.48, 1.88, and 2.35 μm in thulium doped fluorozirconate fiber," Electron. Lett. **25,** 1660-1662 (1989).
2. S. Tanabe, X. Feng, and T. Hanada, "Improved emission of Tm^{3+}-doped glass for a 1.4 μm amplifier by radiative energy transfer between Tm^{3+} and Nd^{3+}," Opt. Lett. **25,** 817-819 (2000).
3. J. Wu, Z. Yao, J. Zong, and S. Jiang, "Highly efficient high-power thulium-doped germanate glass fiber laser," Opt. Lett. **32,** 638-640 (2007).
4. J. S. Wang, E. M. Vogel, and E. Snitzer, "Tellurite glass: a new candidate for fiber devices," Opt. Mater. **3**, 187-203 (1994).
5. R. A. H. El-Mallawany, *Tellurite Glasses Handbook-Physical Properties and Data*, (CRC Boca Raton, FL 2001).
6. S. Q. Man, E. Y. B. Pun, and P. S. Chung, "Tellurite glasses for 1.3 μm optical amplifiers," Opt. Commun. **168**, 369-373 (1999).
7. M. Yamada, A. Mori, K. Kobayashi, H. Ono, T. Kanamori, K. Oikawa, Y. Nishida, Y. Ohishi, "Gain-flattened tellurite-based EDFA with a flat amplification bandwidth of 76 nm," IEEE Photon. Technol. Lett. **10**, 1244-1246 (1998).
8. S. Shen, A. Jha, L. Huang, and P. Joshi, "980-nm diode-pumped Tm^{3+}/Yb^{3+}-codoped tellurite fiber for S-band amplification," Opt. Lett. **30,** 1437-1439 (2005).
9. Aiko Narazaki, Katsuhisa Tanaka, Kazuyuki Hirao, Naohiro Soga, "Induction and relaxation of optical second-order nonlinearity in tellurite glasses," J. Appl. Phys. **85,** 2046-2051 (1999).
10. S. Tanabe, K. Hirao, and N. Soga, "Upconversion fluorescences of TeO_2- and Ga_2O_3-based oxide glasses containing Er^{3+}," J. Non-Cryst. Solids **122**, 79-82 (1990).

#96186 - $15.00 USD Received 13 May 2008; revised 17 Jul 2008; accepted 17 Jul 2008; published 24 Jul 2008

11. Y. Ohishi, A. Mori, M. Yamada, H. Ono, Y. Nishida, and K. Oikawa, "Gain characteristics of tellurite-based erbium-doped fiber amplifiers for 1.5 μm broadband amplification," Opt. Lett. **23**, 274-276 (1998).
12. A. Mori, "1.58-μm Broad-band erbium-doped tellurite fiber amplifier," IEEE J. Lightwave Technol. **LT-20,** 822-827 (2002).
13. R. Balda, J. Fernández, M. A. Arriandiaga, and J. Fernández-Navarro, "Spectroscopy and frequency upconversion in Nd^{3+} doped TeO_2-TiO_2-Nb_2O_5 glass," J. Phys.: Conden. Matter **19**, 086223-086234 (2007).
14. I. Iparraguirre, J. Azkargorta, J. M. Fernández-Navarro, M. Al-Saleh, J. Fernández, and R. Balda, "Laser action and upconversion of Nd^{3+} in tellurite bulk glass," J. Non-Cryst. Solids **353,** 990-992 (2007).
15. B. Richards, Y. Tsang, D. Binks, J. Lousteau, and A. Jha, "Efficient 2 μm Tm^{3+}-doped tellurite fiber laser," Opt. Lett. **33**, 402-404 (2008).
16. N. V. Ovcharenko and T. V. Smirnova, "High refractive index and magneto-optical glasses in the systems TeO_2-WO_3-Bi_2O_3 and TeO_2-WO_3-PbO," J. Non-Cryst. Solids **291,** 121-126 (2001).
17. B. R. Judd, "Optical absorption intensities of rare-earth ions," Phys. Rev. **127**, 750-761 (1962).
18. G. S. Ofelt, "Intensities of crystal spectra of rare-earth ions," J. Chem. Phys. **37**, 511-520 (1962).
19. W. T. Carnall, P. R. Fields, and K. Rajnak, "Spectral Intensities of the trivalent lanthanides and actinides in solution. II. Pm^{3+}, Sm^{3+}, Eu^{3+}, Gd^{3+}, Tb^{3+}, Dy^{3+}, and Ho^{3+}," J. Chem. Phys. **49**, 4412-4423 (1968).
20. V. Dimitrov and T. Komatsu, "Classification of Simple Oxides: A Polarizability Approach," J. Solid State Chem. **163,** 100-112 (2002).
21. R. Balda, J. Fernández, S. García-Revilla, J. M. Fdez-Navarro, "Spectroscopy and concentration quenching of the infrared emission in Tm^{3+}-doped TeO_2-$TiO_2Nb_2O_5$ glass," Opt. Express **15**, 6750-6761 (2007).
22. C. K. Jorgensen and R. Reisfeld, "Judd–Ofelt parameters and chemical bonding," J. Less-Common Met. **93**, 107-112 (1983).
23. G. Özen, A. Aydinli, S. Cenk, and A. Sennarglu, "Effect of composition on the spontaneous emission probabilities, stimulated emission cross-sections and local environment of Tm^{3+} in TeO_2-WO_3 glass," J. Lumin. **101**, 293-306 (2003)
24. M. J. Weber, "Probabilities for radiative and nonradiative decay of Er^{3+} in LaF_3," Phys. Rev. **157**, 262-272 (1967).
25. A. Brenier, C. Pedrini, B. Moine, J. L. Adam, and C. Pledel, "Fluorescence mechanisms in Tm^{3+} singly doped and Tm^{3+}, Ho^{3+} doubly doped indium-based fluoride glasses," Phys. Rev. B **41**, 5364-5371 (1990).
26. M. J. Weber, D. C. Ziegler, and C. A. Angell, "Tailoring stimulated emission cross sections of Nd^{3+} laser glass: Observation of large cross sections for $BiCl_3$ glasses," J. Appl. Phys. **53**, 4344-4350 (1982).
27. M. Naftaly, S. Shen, and A. Jha, "Tm^{3+}-doped tellurite glass for a broadband amplifier at 1.47 μm," Appl. Opt. **39**, 4979-4984 (2000).
28. J. L. Doualan, S. Girard, H. Haquin, J. L. Adam, and J. Montagne, "Spectroscopic properties and laser emission of Tm doped ZBLAN glass at 1.8 μm," Opt. Mater. **24**, 563-577 (2003).
29. M. D. O'Donnell, K. Richardson, R. Stolen, C. Rivero, T. Cardinal, M. Couzi, D. Furniss, and A. B. Seddon, "Raman gain of selected tellurite glasses for IR fibre lasers calculated from spontaneous scattering spectra," Opt. Mater. **30**, 946-951 (2008).
30. M. J. Weber, "Luminescence decay by energy migration and transfer: observation of diffusion-limited relaxation," Phys. Rev. B **4**, 2932-2939 (1971).
31. M. Yokota and O. Tanimoto, "Effects of diffusion on energy transfer by resonance," J. Phys. Soc. Japan **22**, 779-784 (1967).
32. A. I. Burshtein, "Hopping mechanism of energy transfer," Sov. Phys. JETP **35,** 882-885 (1972).
33. Y. S. Han, J. Heo, and Y. B. Shin, "Cross relaxation mechanism among Tm^{3+} ions in $Ge_{30}Ga_2As_6S_{62}$ glass," J. Non-Cryst. Solids **316**, 302-308 (2003).
34. A. Sennaroglu, A. Kurt, and G. Özen, "Effects of cross-relaxation on the 1470 and 1800 nm emissions in Tm^{3+}:TeO_2-$CdCl_3$ glass," J. Phys. Conden. Matter **16**, 2471-2478 (2004).

#96186 - $15.00 USD Received 13 May 2008; revised 17 Jul 2008; accepted 17 Jul 2008; published 24 Jul 2008

1. Introduction

In the last years, Tm^{3+}-doped glasses have generated a great deal of attention due to the interesting spectroscopic properties of their 1.4 μm and 1.8 μm infrared emissions. The $^3H_4 \rightarrow {}^3F_4$ emission at around 1.4 μm is important to achieve a band extension in the spectral range corresponding to the S-band amplifier region, on the short wavelength side of the conventional erbium-doped fiber amplifier C band at 1530-1570 nm. On the other hand, the $^3F_4 \rightarrow {}^3H_6$ transition around 1800 nm is of interest to extend lasing capability into the 1600-1900 nm atmospheric window [1-3]. To develop more efficient optical devices based on Tm^{3+} ions the choice of both the host glass and active ion concentration is very important. The host matrix should have low phonon energy to minimize multiphonon relaxation rates because the energy difference between the $^3H_4$ and the next lower-lying $^3H_5$ is not large (≈4300 cm^{-1}). To avoid this problem, glasses with low phonon energies such as fluorides, chalcogenides, tellurites, and heavy metal oxide glasses are required.

Tellurite glasses have attracted a considerable interest especially because of their high refractive index and low phonon energies [4,5]. Moreover, these glasses combine good mechanical stability, chemical durability, and high linear and nonlinear refractive indices, with a wide transmission window (typically 0.4-6 μm), which make them promising materials for photonic applications such as upconversion lasers, optical fiber amplifiers, non linear optical devices, and so on [6-15]. Broadband Er-doped fiber amplifiers have been achieved by using tellurite-based fibers as the erbium host [11,12] and very recently, efficient laser emission around 2 μm has been demonstrated in a tellurite fiber [15].

Another factor to be considered in achieving amplification in the S-band through the $^3H_4 \rightarrow {}^3F_4$ emission is that this transition is affected by cross-relaxation among Tm^{3+} ions. When the activator ion concentration in glass becomes high enough, ions interact and ion-ion energy transfer occurs. The energy transfer processes reduce the lifetime and consequently the efficiency of the $^3H_4$ level due to the well known cross relaxation process ($^3H_4$, $^3H_6 \rightarrow {}^3F_4$, $^3F_4$) [4]. In this process part of the energy of an ion in the $^3H_4$ level is transferred to another ion in the ground state with both ions ending up in the $^3F_4$ level.

In this work, we have characterized the spectroscopic properties of the infrared $^3H_4 \rightarrow {}^3F_4$ emission of Tm^{3+} ions in two different compositions of TeO_2-WO_3-PbO tellurite glasses for three Tm_2O_3 concentrations (0.1, 0.5, and 1 wt%) by using steady-state and time-resolved laser spectroscopy. These glasses contain oxides of the heaviest metals such as tungsten and lead, which increases the linear and nonlinear refractive indexes [16]. The high linear index increases the local field correction at the rare-earth site leading to large radiative transition probabilities. On the other hand, the presence of two glass formers, such as TeO_2 and WO_3 produces a more complex network structure with a great variety of sites for the RE ions which contributes to the inhomogeneous broadening of the emission bands. The study includes absorption and emission spectroscopy and lifetime measurements for the infrared $^3H_4 \rightarrow {}^3F_4$ emission at different concentrations. The analysis of the fluorescence decays from the $^3H_4$ level indicates the presence of a dipole-dipole quenching process assisted by energy migration. The average critical distance, which indicates the extent to which the energy transfer can occur, has been obtained and compared with other glasses.

2. Experimental techniques

The glasses with mol% compositions $80TeO_2$-$15WO_3$-5PbO (TWP5) and $50TeO_2$-$30WO_3$-20PbO (TWP20) were prepared by melting 10 g batches of high-purity TeO_2 (Sigma-Aldrich 99.995), WO_3 (Aldrich 99.995) and PbO (99.999 Aldrich) reagents in a platinum crucible placed in an electrical Thermostar™ furnace at variable temperatures between 710 and 740º C during 30-45 min. The melts were stirred with a platinum rod and then poured onto a preheated brass plate, annealed 15 min at 390-400º C, and further cooled at a 3º C/min rate down to room temperature. The glasses were doped with different Tm_2O_3 (Aldrich 99.99%)

#96186 - $15.00 USD Received 13 May 2008; revised 17 Jul 2008; accepted 17 Jul 2008; published 24 Jul 2008

concentrations (0.1, 0.5, and 1 wt%). No post-melting analysis was made. The optical measurements were carried out on polished planoparallel glass slabs of about 2 mm thickness.

Conventional absorption spectra were performed with a Cary 5 spectrophotometer. The samples temperature was varied between 10 and 295 K in a continuous flow cryostat. The steady-state emission measurements were made with a Ti-sapphire ring laser (0.4 cm^{-1} linewidth) in the 760-940 nm spectral range as exciting light. The fluorescence was analyzed with a 0.25 monochromator, and the signal was detected by an extended IR Hamamatsu R5509-72 photomultiplier and a PbS detector. Lifetime measurements were obtained by exciting the samples with a Ti-sapphire laser pumped by a pulsed frequency doubled Nd:YAG laser (9 ns pulse width), and detecting the emission with a Hamamatsu R5509-72 photomultiplier. Data were processed by a Tektronix oscilloscope.

3. Experimental results

3.1 Absorption measurements

The room temperature absorption spectra were obtained for all samples in the 300-2000 nm range with a Cary 5 spectrophotometer. As an example, Fig. 1 shows the absorption cross-section as a function of wavelength for the two glasses. The spectra are characterized by the bands corresponding to the transitions starting from the $^3H_6$ ground state to the different higher levels $^1G_4$, $^3F_{2,3}$, $^3H_4$, $^3H_5$, and $^3F_4$. The profile and the position of the absorption bands are similar with slight differences in the absorption cross-section. However, as expected, the optical band gap is shifted to longer wavelengths in the glass with the higher content of WO_3 and PbO. In both glasses, energy levels higher than $^1G_4$ are not observed because of the intrinsic absorption bandgap.

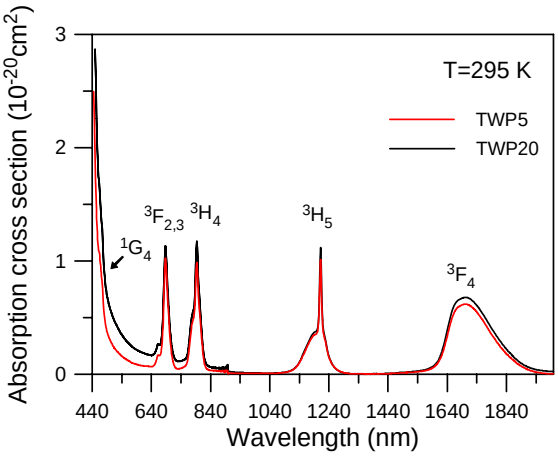

Fig. 1. Room temperature absorption cross-section of Tm^{3+} in TWP5 and TWP20 glasses.

Data from these spectra have been used to calculate the radiative transition rates by using the Judd-Ofelt (JO) theory [17,18]. Five absorption bands ($^3F_{2,3,}$ $^3H_4$, $^3H_5$, and $^3F_4$) were chosen for the calculation. To obtain the contribution to the integrated absorption coefficient corresponding to levels $^3F_2$ and $^3F_3$ a Gaussian fit method has been used to separate the overlapping peaks. The measured absorption bands are all dominated by electric dipole transitions except the transition $^3H_6 \rightarrow {}^3H_5$, which contains electric-dipole and magnetic-dipole contributions. The magnetic-dipole contribution, f_{md}, can be obtained from equation $f_{md}=nf'$ [19], where n is the refractive index of the studied glasses and f´ is a quantity calculated on the basis of energy-level parameters for lanthanide aquo ions. The electric dipole oscillator strength for this transition is then obtained by subtracting the calculated magnetic-dipole contribution from the experimental oscillator strength. The error analysis of the measured

#96186 - $15.00 USD Received 13 May 2008; revised 17 Jul 2008; accepted 17 Jul 2008; published 24 Jul 2008

quantities used in the JO calculation gives an estimated accuracy of 5%. The JO parameters obtained for these glasses together with the density, refractive index, and Tm^{3+} concentration (calculated from the density) for samples with 1 wt% of Tm_2O_3 are displayed in Table 1. As can be seen from this Table the density increases as the WO_3 and PbO content increases due to the higher atomic weight of these oxides compared with TeO_2. The refractive index also increases in the glass with the higher content of WO_3 and PbO due to their higher polarizability compared with TeO_2 [20]. The values for the JO parameters are in agreement with those previously reported in other tellurite glasses [21]. It is well known that Ω_2 is the most sensitive to local structure and glass composition and its value is indicative of the amount of covalent bonding between RE ions and ligand anions [22]. As can be seen in Table 1, Ω_2 is slightly higher for the glass with the higher content of WO_3 and PbO. This behavior can not be explained in terms of covalency because the increase of WO_3 and PbO with strong W-O and Pb-O bonds of highly covalent character should reduce the covalency of the RE ions and therefore the Ω_2 value. The increase of Ω_2 as WO_3 content increases has also been observed in TeO_2-WO_3 binary glasses and related to a larger asymmetry of the local environment of the Tm^{3+} ions in the matrix [23].

Table 1. Density, Tm^{3+} ions concentration, refractive index, JO parameters, and r.m.s. deviation for the two glasses.

Glass	Density (gcm^{-3})	N (cm^{-3})	n	Ω_2 ($x10^{-20}$)	Ω_4 ($x10^{-20}$)	Ω_6 ($x10^{-20}$)	r.m.s.
TWP5	6.08	$1.88x10^{20}$	2.155	4.04	1.55	1.26	$4.89x10^{-7}$
TWP20	6.88	$2.13x10^{20}$	2.175	4.61	1.47	1.29	$4.55x10^{-7}$

The radiative transition probabilities for the excited levels of Tm^{3+} can be calculated by using the JO parameters. The radiative transition probability is given by [24],

$$A[(S,L)J;(S',L')J'] = \frac{64\pi^4 e^2}{3h\lambda^3(2J+1)}\left[n\frac{(n^2+2)^2}{9}S_{ed} + n^3 S_{md}\right] \quad (1)$$

where $n\frac{(n^2+2)^2}{9}$ is the local field correction for electric dipole transitions and n^3 for magnetic dipole transitions.

The radiative lifetime is related to radiative transition probabilities by,

$$\tau_R = \left\{\sum_{S',L',J'} A[(S,L)J;(S',L')J']\right\}^{-1} \quad (2)$$

The fluorescence branching ratio can be obtained from the transition probabilities by using,

$$\beta[(S,L)J;(S',L')J'] = \frac{A[(S,L)J;(S',L')J']}{\sum_{S',L',J'} A[(S,L)J;(S',L')J']} \quad (3)$$

The radiative transition probabilities, the branching ratios, and the radiative lifetimes of some selected levels of Tm^{3+} for both glass compositions are shown in Table 2. Since the radiative transition probability is related to the refractive index of the glass host, the glass with the highest content of PbO, which has a slightly higher refractive index presents higher radiative transition probabilities.

#96186 - $15.00 USD Received 13 May 2008; revised 17 Jul 2008; accepted 17 Jul 2008; published 24 Jul 2008

3.2 Emission and fluorescence lifetimes

The infrared emission in the 1300-2200 nm spectral range was obtained for all samples at room temperature by exciting at 793 nm. As an example, Fig. 2 shows the fluorescence spectra corresponding to the $^3H_4 \rightarrow {}^3F_4$ and $^3F_4 \rightarrow {}^3H_6$ transitions normalized to $^3H_4 \rightarrow {}^3F_4$ transition for the three samples doped with 0.1, 0.5, and 1 wt% of Tm_2O_3 in the two glasses.

Table 2. Predicted radiative transition rates, lifetimes, and branching ratios of some excited levels of Tm^{3+} in TWP glasses.

Transitions	Energies (cm^{-1})	A_{rad} (s^{-1})	τ_{rad} (ms)	β (%)
TWP5				
$^3H_4 \rightarrow {}^3H_6$	12610	3000	0.302	90.6
$^3H_4 \rightarrow {}^3F_4$	6716	252		7.6
$^3H_4 \rightarrow {}^3H_5$	4359	57		1.7
$^3H_5 \rightarrow {}^3H_6$	8251	625	1.58	99
$^3H_5 \rightarrow {}^3F_4$	2430	6.3		1
$^3F_4 \rightarrow {}^3H_6$	5537	512	1.95	100
TWP20				
$^3H_4 \rightarrow {}^3H_6$	12608	3332	0.272	90.8
$^3H_4 \rightarrow {}^3F_4$	6711	279		7.6
$^3H_4 \rightarrow {}^3H_5$	4364	57		1.5
$^3H_5 \rightarrow {}^3H_6$	8243	672	1.47	99
$^3H_5 \rightarrow {}^3F_4$	2797	6.4		1
$^3F_4 \rightarrow {}^3H_6$	5491	571	1.75	100

In both glasses, the spectra show a strong emission band centered around 1490 nm which corresponds to the $^3H_4 \rightarrow {}^3F_4$ transition together with a less intense emission band centered around 1820 nm and corresponding to the $^3F_4 \rightarrow {}^3F_6$ transition. The relative intensity ratio between the 1490 nm and 1820 nm emissions decreases as the Tm^{3+} concentration increases up to 1wt%. This reduction of the $^3H_4 \rightarrow {}^3F_4$ emission intensity with concentration had been previously observed and attributed to cross-relaxation between $^3H_4 \rightarrow {}^3F_4$ and $^3H_6 \rightarrow {}^3F_4$ transitions [4,25].

#96186 - $15.00 USD Received 13 May 2008; revised 17 Jul 2008; accepted 17 Jul 2008; published 24 Jul 2008

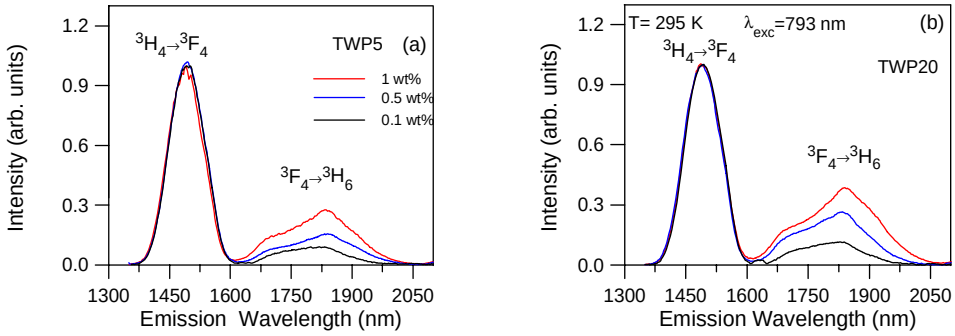

Fig. 2. Room temperature emission spectra of Tm^{3+} in TWP5 (a) and TWP20 (b) glasses for three Tm_2O_3 different concentrations.

The room temperature stimulated emission cross section of the $^3H_4 \rightarrow {}^3F_4$ laser transition has been obtained by using the following expression [26],

$$\sigma_{se} = \frac{\lambda_p^4}{8\pi n^2 c} \frac{\beta}{\tau_R \Delta\lambda_{eff}} \tag{4}$$

where λ_p is the peak fluorescence wavelength, β is the branching ratio for the transition, n is the index of refraction of the host matrix, c the velocity of light, τ_R the radiative lifetime of the emitting level, and $\Delta\lambda_{eff}$ is the effective linewidth. The effective linewidth of the transition has been calculated by using the relation $\Delta\lambda_{eff} = \int \frac{I(\lambda)d\lambda}{I_{max}}$. The effective linewidth values are 101 and 102 nm for TWP5 and TWP20 glasses respectively. It is broader by nearly 30 nm in these glasses if compared to fluoride ones which makes them attractive for broadband amplifiers specially in the wavelength range that overlaps the conventional band of erbium doped fiber amplifiers. The maximum emission cross-section values are 0.38×10^{-20} cm^2 and 0.40×10^{-20} cm^2 for TWP5 and TWP20 glasses respectively, which are similar to those found in other tellurite glasses and twice the one of ZBLAN glass [27]. The gain bandwidth of an amplifier is determined by the product of the width of the emission spectrum and the emission cross-section. The obtained values for this product in these glasses are more than twice larger than in fluoride glass which suggests that these glasses may provide extended short wavelength gain of the erbium-doped C band at 1530-1570 nm. As an example, Fig. 3 shows the spectral overlap between the normalized $^3H_4 \rightarrow {}^3F_4$ and $^4I_{13/2} \rightarrow {}^4I_{15/2}$ emissions of Tm^{3+} and Er^{3+} ions respectively together with the emission spectrum of a codoped sample with 0.3 wt% Tm_2O_3 and 0.3 wt% Er_2O_3 for TWP20 glass. As can be seen, a broad emission from 1400 to 1680 nm with a full width at half-maximum of ~ 180 nm is obtained by codoping the glass which suggests that these glasses could be promising materials for broadband light sources and broadband amplifiers for wavelength-division-multiplexing (WDM) transmission systems.

#96186 - $15.00 USD Received 13 May 2008; revised 17 Jul 2008; accepted 17 Jul 2008; published 24 Jul 2008

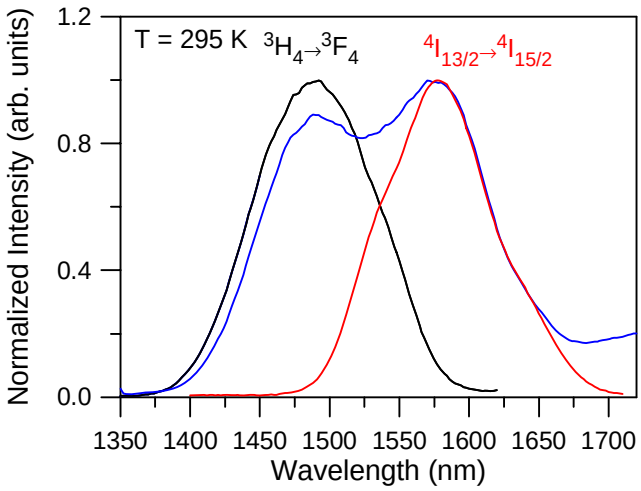

Fig. 3. Spectral overlap between the $^3H_4 \rightarrow {}^3F_4$ (black) and $^4I_{13/2} \rightarrow {}^4I_{15/2}$ (red) normalized emissions of Tm^{3+} and Er^{3+} ions respectively in TWP20 glass together with the emission spectrum of a codoped sample (blue).

We have also obtained the room temperature stimulated emission cross section of the $^3F_4 \rightarrow {}^3H_6$ laser transition by using expression (4). In this case, for an emission between the first excited level and the ground state the branching ratio is equal to unity. The maximum emission cross sections are 0.85×10^{-20} cm^2 and 0.94×10^{-20} cm^2 for TWP5 and TWP20 glasses respectively. As for the $^3H_4 \rightarrow {}^3F_4$ transition, this value is twice the one of ZBLAN glass [28].

The fluorescence lifetimes of level $^3H_4$ were measured as a function of temperature by exciting the samples at 793 nm. The observed behavior is similar in both glasses. At low concentration and temperature, the lifetime is close to the calculated radiative lifetime; however, as concentration increases, the lifetimes decrease even at low temperature, which indicates the presence of nonradiative energy transfer processes.

The fluorescence decays for the samples doped with 0.1 and 0.5% of Tm_2O_3 can be described at all temperatures by an exponential function to a good approximation; however, for the samples doped with 1 wt% the decays become non exponential. As an example, Fig. 4 shows the logarithmic plot of the experimental decays of the $^3H_4$ level at 295 K for the samples doped with 0.1, 0.5, and 1 wt% for both glasses.

#96186 - $15.00 USD Received 13 May 2008; revised 17 Jul 2008; accepted 17 Jul 2008; published 24 Jul 2008

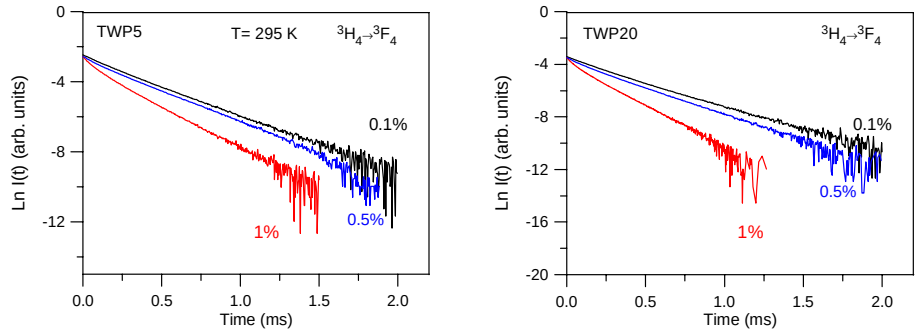

Fig. 4. Logarithmic plot of the fluorescence decay of the $^3H_4$ level obtained under excitation at 793 nm at room temperature for TWP5 and TWP20 glasses doped with 0.1, 0.5, and 1 wt%.

Figure 5 shows the lifetime values of the $^3H_4$ level between 10 K and 295 K for the samples doped with 0.1, 0.5, and 1 wt% for both glasses. The lifetime values for the samples doped with 1 wt% correspond to the average lifetime defined by $\langle \tau \rangle = \frac{\int I(t)dt}{I_0}$.

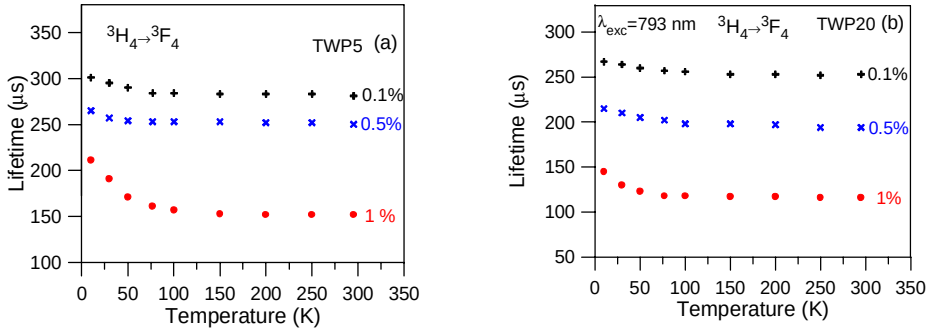

Fig. 5. Temperature dependence of the $^3H_4$ level lifetime for different Tm_2O_3 concentrations in TWP5 (a) and TWP20 (b) glasses.

3.3 Concentration quenching of the $^3H_4$ emission

As we mentioned before the relative intensity ratio between the 1490 nm and 1820 nm emissions decreases as Tm^{3+} concentration increases. This concentration quenching is also made evident by the change from exponential to non-exponential decays of level $^3H_4$ and the lifetime reduction and can be attributed to cross-relaxation processes such as $^3H_4$, $^3H_6 \rightarrow {}^3F_4$, $^3F_4$. In this process part of the energy of an ion in level $^3H_4$ is transferred to another ion in the ground state with both ions ending up in level $^3F_4$ [4]. This process reduces the lifetime of the $^3H_4$ level and consequently the efficiency of the 1490 nm emission.

The characteristic decay time of the $^3H_4$ level should be governed by a sum of probabilities for several competing processes: radiative decay, nonradiative decay by multiphonon relaxation and by energy transfer to other Tm^{3+} ions. In these tellurite glasses nonradiative decay by multiphonon relaxation is expected to be small because of the 4300 cm^{-1} energy difference between $^3H_4$ and $^3H_5$ levels and the energy of the phonons involved. According to

#96186 - $15.00 USD Received 13 May 2008; revised 17 Jul 2008; accepted 17 Jul 2008; published 24 Jul 2008

the literature, the highest phonons energy of tungsten-tellurite glasses is about 920 cm^{-1} [29]. This corresponds to 4.6 phonons, and indicates that the magnitude of the multiphonon relaxation rate is small. Energy transfer processes such as cross-relaxation are generally described in terms of three limiting cases: (i) direct relaxation, (ii) fast diffusion, and (iii) diffusion limited relaxation [30]. In the case of very fast diffusion, the decay of the donor fluorescence is purely exponential; however, as we have seen in Fig. 4 the decays become non exponential for the samples doped with 1 wt% of Tm_2O_3. The analysis of these decay curves shows that energy migration among Tm^{3+} ions affects the energy transfer process. The fit of the fluorescence decays with the migration assisted energy transfer models from Yokota and Tanimoto and Burshtein [31,32] indicates that the best agreement between experimental data and theoretical fits is obtained with the expression corresponding to the Burshtein model,

$$I(t) = I_0 \exp\left(-\frac{t}{\tau_R} - \gamma\sqrt{t} - Wt \right) \tag{5}$$

where τ_R is the intrinsic lifetime of donor ions, γ characterizes the direct energy transfer, and W represents the migration parameter. In the case of dipole-dipole interaction, γ is given by the expression $\gamma = \frac{4}{3}\pi^{3/2} N\, C_{DA}^{1/2}$, where N is the concentration and C_{DA} is the energy transfer microparameter. Figure 6 shows the fit for the samples doped with 1 wt% at room temperature.

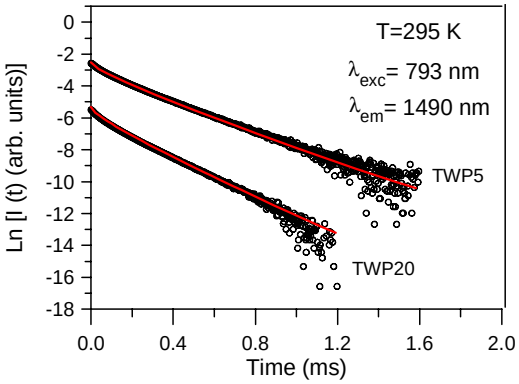

Fig. 6. Experimental emission decay curves of level $^3H_4$ for TWP5 and TWP20 glasses doped with 1 wt% Tm_2O_3 at room temperature and the calculated fit with Eq. (5) (solid line).

These results indicate that the electronic mechanism of energy transfer is a dipole-dipole interaction in the framework of a diffusion-limited regime. The values obtained for the energy transfer microparameter and the migration transfer rate for both glasses are shown in Table 3 together with the critical distance R_0 calculated by $R_0^6 = \tau_R C_{DA}$. The critical distance for energy transfer is defined as the distance at which the energy transfer probability becomes equal to the intrinsic decay rate of the metastable level and indicates the extent to which the energy transfer between ions can occur. The obtained values for the critical distance and the migration transfer rate are slightly higher for TWP20 glass which have a higher concentration of Tm^{3+} ions. The critical distance in these glasses is similar to the one reported in other tellurite glasses [21], larger than in chalcogenide glass (7.3 Å) [33], and much shorter than the value reported in TeO_2-$CdCl_2$ glass [34].

#96186 - $15.00 USD Received 13 May 2008; revised 17 Jul 2008; accepted 17 Jul 2008; published 24 Jul 2008

Table 3. Obtained values for the energy transfer microparameter, migration transfer rate, and critical distance for the two glasses doped with 1 wt% at room temperature.

Glass	N (cm^{-3})	C_{DA} (cm^6/s)	W (s^{-1})	R_0 (Å)
TWP5	$1.88x10^{20}$	$1.06x10^{-39}$	628	8.3
TWP20	$2.13x10^{20}$	$1.63x10^{-39}$	1150	8.7

4. Conclusions

Absorption and luminescence measurements have been performed in Tm^{3+} doped $80TeO_2$-$15WO_3$-5PbO and $50TeO_2$-$30WO_3$-20PbO tellurite glasses. The Judd-Ofelt intensity parameters and radiative transition rates have been calculated. The glass with the highest content of WO_3 and PbO, which has a slightly higher refractive index presents higher radiative transition probabilities and shorter radiative lifetimes.

The infrared emission at around 1490 has been characterized for three Tm_2O_3 concentrations (0.1, 0.5, and 1 wt%). Fluorescence measurements show that in both glasses the 1490 nm emission presents two noticeable features if compared to fluoride glasses. On one hand, it is broader by nearly 30 nm, and on the other, the stimulated emission cross section is twice the value for fluoride glasses. These features make these glasses attractive for broadband amplifiers specially in the wavelength range that overlaps the conventional band of the erbium doped fiber amplifier. In fact, we have shown that with an Tm^{3+}-Er^{3+} codoped sample a broad emission band with an effective linewidth of around 180 nm can be obtained in these glasses.

The relative intensity ratio between the $^3H_4 \rightarrow {}^3F_4$ and $^3F_4 \rightarrow {}^3H_6$ emissions and the measured lifetime of the $^3H_4$ level decreases as thulium concentration increases, due to the presence of cross-relaxation processes. An analysis of the fluorescence decays of the $^3H_4 \rightarrow {}^3F_4$ emission as a function of concentration reveals that a dipole-dipole quenching process assisted by energy migration is consistent with the experimental results.

Acknowledgments

This work was supported by the Spanish Government MEC (MAT2005-06508-C02-02) and the Basque Country Government (IT-331-07).

#96186 - $15.00 USD Received 13 May 2008; revised 17 Jul 2008; accepted 17 Jul 2008; published 24 Jul 2008